

Carbon materials for drug delivery & cancer therapy

Carbon nanotubes and graphene are both low-dimensional sp^2 carbon nanomaterials exhibiting many unique physical and chemical properties that are interesting in a wide range of areas including nanomedicine. Since 2004, carbon nanotubes have been extensively explored as drug delivery carriers for the intracellular transport of chemotherapy drugs, proteins, and genes. *In vivo* cancer treatment with carbon nanotubes has been demonstrated in animal experiments by several different groups. Recently, graphene, another allotrope of carbon, has also shown promise in various biomedical applications. In this article, we will highlight recent research on these two categories of closely related carbon nanomaterials for applications in drug delivery and cancer therapy, and discuss the opportunities and challenges in this rapidly growing field.

Zhuang Liu^{*a}, Joshua T. Robinson^b, Scott M. Tabakman^b, Kai Yang^a, and Hongjie Dai^{*b}

^aJiangsu Key Laboratory for Carbon-Based Functional Materials & Devices, Institute of Functional Nano & Soft Materials, Soochow University, Suzhou, Jiangsu, 215123, China

^bDepartment of Chemistry, Stanford University, Stanford, California, 94304, USA

*E-mail: zliu@suda.edu.cn, hdai@stanford.edu

In the past decade, the rapid development of nanotechnology has brought many fascinating ideas and opportunities to disease diagnosis and treatment. sp^2 carbon nanomaterials, notably zero-dimensional (0D) fullerenes, 1D carbon nanotubes (CNTs), and 2D graphene, have gained significant interest from various fields and generated huge impacts in the materials research community since their discovery in 1985, 1991, and 2004, respectively¹⁻³. Graphene is a mono-layered sp^2 -bonded carbon sheet. Single-walled carbon nanotubes (SWNTs) and multi-walled carbon nanotubes (MWNTs) are cylindrical tubes of sp^2 carbon, conceptualized by rolling up single- or multi-layered graphene, respectively. Potential

applications of these carbon nanomaterials span disciplines including nano-electronics, composite materials, energy research, and biomedicine⁴⁻⁹.

Fullerenes and their derivatives can serve as drug delivery vehicles, and in certain circumstances, as nano-drugs by themselves¹⁰⁻¹². CNTs have been developed as novel biosensing platforms to detect different biological targets and as nano-probes for biomedical imaging^{8,13,14}. Functionalized CNTs can be used as molecular carriers for *in vitro* and *in vivo* drug delivery, and have been primarily employed for applications in cancer treatment⁸. Recently, graphene, a rising star in the materials science community, has also attracted increasing interest

in biomedicine^{9,14-17}. Herein, we focus on carbon nanotubes and graphene for drug delivery and cancer treatment. *In vitro* cell uptake and intracellular molecular transport with CNTs are initially discussed. Encouraging *in vitro* results prompted further research of CNT-based drug delivery for *in vivo* cancer treatment. Recent progress on using graphene in the field of drug delivery is also reviewed. In addition to the delivery of therapeutic molecules, carbon nanotubes and graphene demonstrate strong optical absorption in the near-infrared (NIR) region, making them promising materials for use in the photothermal ablation of tumors. Despite the encouraging pre-clinical results shown by various groups, several obstacles must be overcome before these carbon nanomaterials can be put to clinical use. To conclude, the future challenges and prospects of using CNTs and graphene in nanomedicine, as well as the comparison between them, will be addressed.

Interactions of carbon nanotubes with cells

Motivated by the unique 1D structure of CNTs, a number of groups explored the possible entry of nanotubes into cells as early as 2004¹⁸⁻²⁰. Numerous reports have shown that functionalized, water-soluble CNTs are able to enter cells, although the exact uptake mechanism for CNTs may depend on the size and surface chemistry. The majority of studies over the past several years have uncovered that CNTs functionalized by oxidization, wrapped by DNA, and coated by surfactants or amphiphilic polymers are able to be engulfed by cells via the energy-dependent endocytosis pathway^{8,20-26}. This entryway is similar to many other nanomaterials used in biomedicine. However, it has also been reported that CNTs functionalized by the 1,3-dipolar cycloaddition, or Prato reaction, entered cells by passive diffusion owing to the needle-like structure of nanotubes^{19,27,28}. Besides surface chemistry, the size of CNTs plays an important role in their interaction with cells. A recent study uncovered that the endocytosis pathway for 100 – 200 nm SWNTs was mainly through clathrin-coated pits, but shorter SWNTs (50 – 100 nm) were internalized through clathrin-coated vesicles as well as the caveolae pathway²⁹. Work by Yan and co-workers proposed that individual MWNTs could enter cells through direct penetration while MWNT bundles are taken up by cells through endocytosis³⁰.

After endocytosis CNTs were mainly located inside cell endosomes and lysosomes. Whether CNTs can escape from these membrane-bound compartments inside cells may also depend on the sizes and surface coating. While SWNTs functionalized by DNA or PEG are mostly retained inside endosomes and lysosomes^{22,23,31-33}, it has been found that individualized MWNTs were able to travel through various cellular barriers and even entered the nucleus^{28,30}. In a recent work, Zhou *et al.* found that by conjugating different molecules to PEG-functionalized SWNTs, nanotubes were able to localize in specific sub-cellular organelles such as mitochondria³⁴.

The possibility and mechanism of CNTs escaping from cells after cellular uptake is another important question. By using the intrinsic

photoluminescence of SWNTs to track nanotubes inside cells, Jin *et al.* discovered that DNA-coated SWNTs could undergo exocytosis after entering cells via endocytosis²³. Interestingly, the rate of exocytosis was again closely related to the length of the nanotubes, showing slower cellular expulsion for longer nanotubes³⁵. Obviously, the surface chemistry and sizes of CNTs play critical roles in regulating the interactions of CNTs with cells. It is thus crucial to correctly select and control the surface coatings, diameters, and lengths of CNTs to achieve specific aims in CNT-based biomedical applications.

Carbon nanotubes in animals

In the past several years, there have been numerous papers that studied the behavior of carbon nanotubes in animals. The *in vivo* pharmacokinetics, biodistribution, long-term fate, and toxicology of CNTs, which are closely associated with their surface chemistries, sizes, doses, and administration routes, are rather complicated issues, and thus not the focus of this current review article³⁶⁻⁴¹. Although there are certain debates on the clearance mechanism of nanotubes, the majority of studies have suggested that functionalized CNTs, when intravenously injected into animals (e.g., mice, rats), tended to accumulate in the reticuloendothelial system including the liver and spleen, and were gradually excreted, likely via both fecal and renal excretion^{39,42-47}. Recent work by our group investigated the behavior of SWNTs *in vivo* at early time points after intravenous injection. The SWNTs were tracked using their intrinsic near-infrared photoluminescence (NIR PL) for several minutes after injection. Utilizing principle component analysis (PCA), our group was able to identify the time course of SWNTs through individual organs, including the liver, lungs, spleen, and kidneys⁴⁸.

Toxicity is a major concern in using CNTs for biomedical applications. Orally-fed CNTs suspended by surfactants appeared to be safe even at an ultra-high dose of up to 1000 mg/kg⁴⁴. Intratracheal administration of unfunctionalized CNTs aggregated in the lungs and led to pulmonary toxicity and inflammation. This aggregation, however, was not seen for well-dispersed, individualized SWNTs^{43,49-51}. Intraperitoneally injected, large MWNTs, and SWNT bundles induced inflammation and granuloma formation, which again was not found for small MWNTs and individualized SWNTs^{44,52}. Compared with non-functionalized, raw CNTs, well-functionalized CNTs with biocompatible coatings (e.g., by PEGylation) exhibited remarkably reduced *in vivo* toxicity after being intravenously injected into animals^{38,39,53,54}. How CNTs affected the fertility⁵⁵ and induced immune responses^{56,57} after administration to animals has only been partially studied and needs future attention.

Delivery of small drug molecules by carbon nanotubes

Drug delivery is one of the most extensively explored applications of CNTs in biomedicine. In recent years, different strategies have

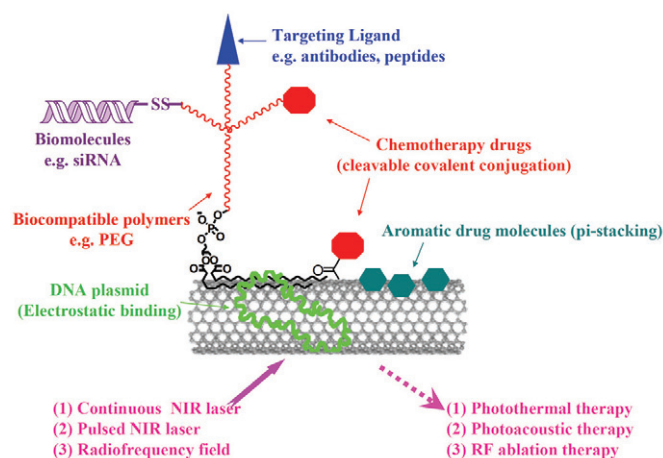


Fig. 1 A schematic drawing showing various approaches for CNT-based drug delivery and cancer therapies.

been developed by various groups to load small molecules such as chemotherapeutic cancer drugs on CNTs via either covalent conjugation or non-covalent adsorption (Fig. 1). Theoretical modeling has also been used to guide the design of CNT-based drug carriers^{58–61}. Covalently conjugated drug molecules are linked to the functional groups on the CNT surface or to the polymer coating of CNTs, usually via cleavable bonds. Anti-cancer or anti-fungal drugs were linked by 1,3-dipolar cycloaddition to functionalized CNTs via amide bonds for drug delivery^{62,63}. The Lippard group and our group used non-covalently PEGylated SWNTs as a longboat delivery system for intracellular transportation of a platinum(IV) complex, which was then reduced to cytotoxic platinum(II) after endocytosis for cancer cell destruction^{64,65}. Other chemotherapeutics such as paclitaxel and cisplatin have been covalently conjugated to CNTs for *in vitro* and *in vivo* drug delivery^{45,66,67}.

Besides covalent linkage, aromatic molecules with a flat structure can be adsorbed on the surface of CNTs via non-covalent π - π stacking. In 2007, our group discovered that doxorubicin, a commonly used cancer chemotherapy drug, could be stacked on the surface of PEGylated SWNTs with a remarkably high loading capacity of up to 4 grams of drug per 1 gram of nanotubes (Fig. 2a), owing to the ultra-high surface area of SWNTs⁶⁸. The pH-dependent drug binding and releasing behaviors are favorable for drug release in endosomes and lysosomes, as well as in tumor micro-environments with acidic pH. This π - π stacking based drug loading strategy was applied to MWNTs and nano-graphene in other studies^{15,16,69,70}.

Following the successful use of CNTs for *in vitro* drug delivery, CNT-based drug carriers have been further utilized for *in vivo* cancer treatment in animal models. In 2008, our group, for the first time, reported *in vivo* cancer treatment using paclitaxel (taxol) conjugated branched PEG-functionalized SWNTs in a 4T1 murine breast cancer model⁶⁶. Compared to free taxol, the SWNT-paclitaxel complex offered improved treatment efficacy, a result of the increased drug

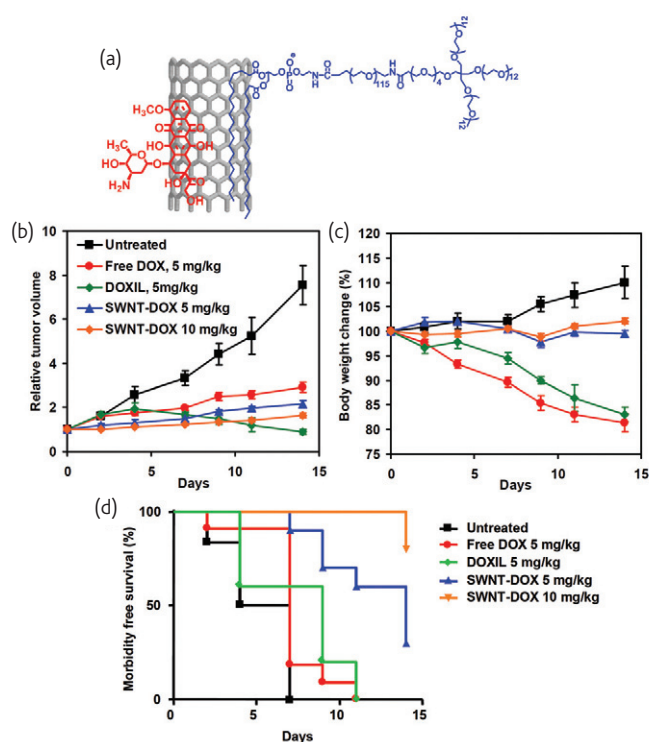


Fig. 2 *In vivo* doxorubicin delivery with carbon nanotubes for cancer treatment. (a) A scheme showing supramolecular π - π stacking of DOX on PEGylated SWNTs. (b–d) Raji tumor bearing SCID mice were treated with different DOX formulations once per week at day 0 and day 7. (b) Tumor sizes of untreated ($n = 7$), 5 mg/kg free DOX treated ($n = 10$, 2 mice died in the second week), 5 mg/kg Doxil treated ($n = 5$), 5 mg/kg SWNT-DOX treated ($n = 10$) and 10 mg/kg SWNT-DOX treated ($n = 10$) mice were measured. (c) SWNT-DOX resulted in far less weight loss than DOX and DOXIL. Averaged tumor volumes and body weights were normalized to day 0. (d) Kaplan–Meier analysis of morbidity free animal survival post various treatments indicated P values: DOX 5 mg/kg versus SWNT-DOX 5 mg/kg or 10 mg/kg, $p < 0.001$; DOXIL 5 mg/kg versus SWNT-DOX 5 mg/kg, $p = 0.013$; DOXIL 5 mg/kg versus SWNT-DOX 10 mg/kg, $p < 0.001$. Error bars in (b,c) were based on the standard error of the mean. Reprinted from⁷¹. © Wiley-VCH Verlag GmbH & Co. KGaA. Reproduced with permission.

accumulation in the tumor due to the enhanced permeability and retention (EPR) effect of cancerous tumors. In a later work, we demonstrated that PEGylated SWNTs loaded with doxorubicin by π - π stacking could also be used for *in vivo* cancer treatment in a Raji B-cell lymphoma model⁷¹. The SWNT-DOX complex, while only exhibiting marginally improved tumor growth inhibition compared with free DOX, was much less toxic to the treated mice, thus offering a remarkably improved therapeutic outcome (Fig. 2). Several other teams have also independently reported CNT-based drug delivery for *in vivo* cancer therapy in animal models. Wu *et al.* demonstrated that MWNTs covalently conjugated with 10-hydroxycamptothecin (HCPT) via a cleavable ester linkage showed superior anti-tumor efficacy than the clinical HCPT formation in a hepatic tumor mouse model⁷².

The aforementioned *in vivo* cancer treatment studies evaluating CNT-drug conjugates were all based on the passive tumor targeting effect of

nanotubes exhibiting long circulation times via the EPR effect. Cancer cell-specific drug delivery with 'smart' targeted CNT bioconjugates (e.g., coupled to targeting ligands) has been widely demonstrated in many *in vitro* experiments^{65,68,73}. We and others have also shown that CNTs conjugated with targeting ligands, including peptides and antibodies, exhibited enhanced tumor uptake compared to non-targeted nanotubes⁷⁴⁻⁷⁶. Notably, *in vivo* tumor targeted drug delivery with CNTs has been rarely reported in animal studies, except for two related studies by Bhirde *et al.*^{45,67}. In their work, SWNTs with or without PEGylation were co-conjugated with cisplatin and epidermal growth factor (EGF) for *in vivo* targeted cancer treatment. Compared with the non-targeted SWNT-cisplatin conjugate, the targeted SWNT-cisplatin-EGF conjugate exhibited an improved tumor growth inhibition effect to the EGF receptor (EGFR) positive head and neck squamous cell carcinoma (HNSCC) tumors, owing to specific EGF-EGFR binding, which enhanced the tumor uptake of nanotube-delivered drugs. Despite their preliminary success, actively tumor-targeted drug delivery with 'smart' CNT bioconjugates, which likely may offer improved clinical efficacy than non-targeted CNTs, are relatively more complicated in terms of fabrication and generalization.

Delivery of biomacromolecules by carbon nanotubes

Differing from small drug molecules which are usually able to diffuse across cell membranes, biomacromolecules such as proteins, DNA, and RNA cannot penetrate the cell membrane by themselves, instead requiring delivery vehicles to help in their cellular entry. Transportation of proteins into cells via CNTs was achieved in a few early reports, where it was shown that proteins could either be conjugated or non-covalently adsorbed on CNTs for intracellular delivery^{20,22,32}. The latter method used the hydrophobic surface of partially functionalized SWNTs (i.e., oxidized SWNTs) for the non-specific binding of proteins. However, proteins transported into cells by CNTs were not effectively released from endosomes, unless an endosome disrupting agent was used³², limiting the applications of CNT-based protein delivery. This approach has not yet been applied in animal studies.

The development of non-viral, biocompatible vectors for efficient intracellular transfection of nucleic acid such as DNA and RNA is one of the most critical challenges toward realizing gene therapy. Several early studies showed that functionalized CNTs with amine groups on their surface were positively charged and able to bind DNA plasmids for gene transfection^{18,77}. However the transfection efficiency of those CNTs appeared to be lower than that of commercial transfection agents such as lipofectamine. To improve their gene delivery ability, cationic polymers including polyethylenimine (PEI) were coupled to CNTs to enhance DNA binding and intracellular trafficking, as well as to induce the endosomal release of DNA⁷⁸⁻⁸⁰. Several latter formulations of CNT-based gene vectors showed comparable or even higher transfection efficiency together with reduced cytotoxicity compared with PEI itself and commercial agents^{79,80}.

Besides DNA plasmids, small interfering RNA (siRNA) that silences specific gene expression can also be delivered into cells by CNTs for RNA interference (RNAi). It has been shown that functionalized CNTs with positive charges (e.g., coated with cationic polymers) could bind siRNA via electrostatic interaction for intracellular transfection⁸¹. Utilizing a cleavable disulfide bond linkage between the siRNA and single-walled CNTs, we successfully delivered siRNA into cells by CNTs and observed gene silencing effects^{33,82}. Interestingly, the SWNT-based siRNA delivery was applicable to hard-to-transfect human T cells and primary cells, which were resistant to conventional cationic liposome-based transfection agents⁸². The CNT-based siRNA transfection has been further demonstrated in animal experiments for *in vivo* gene therapy, showing a tumor growth suppression effect after intratumoral injection of therapeutic CNT-siRNA complexes^{81,83}.

Physical therapies of cancer introduced by carbon nanotubes

The unique physical properties of CNTs are advantageous for use in novel cancer therapies. Both MWNTs and SWNTs exhibit strong optical absorption in the near-infrared (NIR) regions. Upon irradiation by NIR light (700 – 1000 nm), which is a tissue transparency window ideal for optical imaging and phototherapies, CNTs generated heat by light absorption and induced thermal destruction of cancer cells containing significant concentrations of CNTs. In 2005, our group demonstrated *in vitro* targeted photothermal ablation of cancer cells using SWNTs³¹. In this study, PEGylated SWNTs conjugated with folate acid were able to selectively target cancer cells over-expressing the folate receptor, which were thermally destroyed after being exposed to an 808 nm NIR laser at a power density of 2 W/cm². A later work by Chakravarty *et al.* used antibody conjugated SWNTs for photothermal ablation of tumor cells *in vitro*⁸⁴. Recently, a number of other groups have also reported *in vitro* photothermal therapy using CNTs in various different cell line models⁸⁵⁻⁸⁷.

CNT-based photothermal therapy has been further realized in a few animal experiments. Ghosh *et al.* showed that a single treatment consisting of intratumoral injection of DNA-coated MWNTs (100 μ L, 500 μ g/mL) followed by 1064 nm laser irradiation at a power of 2.5 W/cm² completely eliminated PC3 xenograft tumors in 8/8 (100 %) of nude mice, while the growth of control tumors receiving only MWNT injection or laser treatment alone were not affected⁸⁸. In another work by Burke *et al.*, intratumorally injected MWNTs enabled ablation of kidney tumor xenografts with a single NIR laser treatment (1064 nm, 3 W/cm², 30 s), resulting in complete ablation of tumors and an animal survival ratio of 80 % > 3.5 months post treatment with 100 μ g of MWNTs⁸⁹. SWNTs were also used for *in vivo* photothermal treatment of tumors by Moon *et al.*⁹⁰ In their work, carcinoma xenografts growing on nude mice were ablated after being directly injected with PEGylated SWNTs and subsequently exposed to an 808 nm laser. It was found that SWNTs injected into tumors accumulated in the nearby muscle and skin after

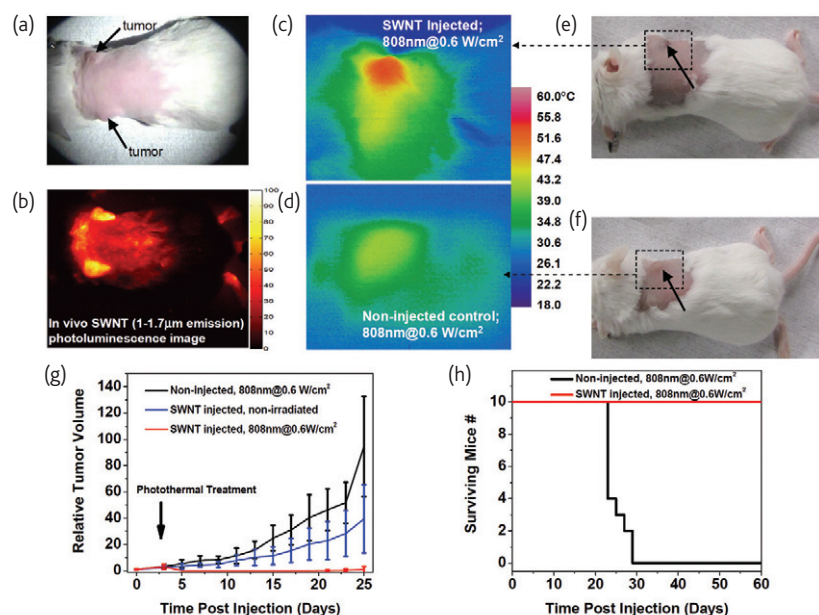


Fig. 3 NIR fluorescence imaging guided photothermal therapy with SWNTs. (a) A digital photo and (b) a NIR photoluminescence image of a BALB/c mouse with two 4T1 tumors (indicated by arrows) taken after intravenous injection of PEGylated SWNTs. IR thermal images of tumor-bearing mice (c) with and (d) without injection of SWNTs under 808 nm laser irradiation for 4.5 minutes (0.6 W/cm^2). (e, f) The corresponding photos of mice before the NIR irradiation. (g) Tumor growth curves and (h) animal survival curves of 4T1 tumor bearing mice after SWNT-based photothermal therapy. 4T1 tumor bearing mice with or without SWNT injection (3.6 mg/kg) were exposed to the 808 nm laser at 0.6 W/cm^2 power for 5 min. All mice from the treatment group were surviving and tumor-free at the end of two months. © 2010. Reproduced with kind permission from Springer Science+Business Media and Tsinghua Press⁹¹.

tumors were destroyed, and then slowly translocated into the liver and spleen, from which nanotubes were gradually excreted.

Those successful demonstrations of using CNTs for *in vivo* photothermal treatment of cancer were all based on the local injection of nanotube solutions directly into tumors. Recently, our groups have achieved photothermal ablation of tumors in mice upon systemic administration of functionalized SWNTs via intravenous injection. By finely tuning the degree of nanotube surface PEGylation, an optimal surface coating of SWNTs was achieved, affording nanotubes with a reasonably long blood circulation half-life of ~12 hours, relatively low accumulation in the reticuloendothelial system organs and the skin, and high uptake in the tumor. *In vivo* photothermal tumor ablation was then achieved using the optimized SWNT conjugate after intravenous injection of nanotubes followed by NIR laser irradiation (808 nm, 2 W/cm^2 , 5 min)³⁶. A separate work demonstrated the dual application of intravenously-injected SWNTs as photoluminescent agents for *in vivo* tumor imaging and as NIR absorbers for photothermal tumor elimination (Fig. 3)⁹¹. Remarkably, successful tumor ablation efficacy was realized using a rather low dose of SWNTs, and a low laser irradiation power ($70 \mu\text{g}$ of SWNT/mouse, laser power 0.6 W/cm^2). Side-by-side experiments were carried out to compare the photothermal treatment performance between SWNTs and gold nanorods (AuNRs), which have been widely used for photothermal tumor therapy. Efficient tumor elimination with SWNTs was achieved at 10 times lower injected doses and lower irradiation powers than for AuNRs ($700 \mu\text{g}$ of AuNR/mouse, laser power 2 W/cm^2). These results highlight the promise

of utilizing the intrinsic optical properties of SWNTs for highly effective *in vivo* imaging-guided photothermal cancer therapy.

Several other CNT-based photo-therapies have also been reported. The photoacoustic effect of CNTs, which has shown great promise as a contrast agent for photoacoustic molecular imaging *in vivo*⁷⁵, can also be utilized for a therapeutic purpose. In an interesting work by Kang *et al.*⁹², a 1064 nm Q-switched millisecond pulsed laser was used to irradiate SWNTs in water, triggering a firecracker-like explosion at the nanoscale to destruct cancer cells. Unlike photothermal therapy that uses heat to 'cook' cancer cells, the temperature change inside cells was insignificant. Using this SWNT-based photoacoustic 'bomb' approach, a remarkably reduced laser power (150 – 1500 times lower than that of photothermal therapy) was sufficient to kill cancer cells. The photothermal effect of CNTs have also been used to enhance intracellular drug delivery. Levi-Polyachenko *et al.* demonstrated that cell membrane permeability could be increased due to the photothermal heating of MWNTs in close proximity to cell membranes, enhancing the delivery of chemotherapeutic drugs into treated cancer cells⁹³.

The major limitation of any photo-therapy is the absorption and scattering of light by biological tissues, even when NIR light is used. Gannon *et al.* discovered that SWNTs were able to generate heat in a 13.6 MHz radiofrequency (RF) field, which had excellent tissue penetration ability⁹⁴. The RF-induced SWNT heating was then used to ablate cancer cells *in vitro* and xenograft tumors growing on rabbits *in vivo*. RF ablation therapy with SWNTs could overcome the limitation of photo-therapies and may be used to treat large or internal tumors.

However, there has not been any follow-up study since the first report in 2007. More efforts are required to further explore the potential of this interesting cancer treatment technique.

Graphene for drug delivery and cancer treatment

Graphene is an sp^2 -bonded carbon sheet with unique physical and chemical properties which has attracted tremendous attention since 2004³. Since 2008, increasing numbers of reports have explored the potential of graphene for different biomedical applications^{9,15,16,95}. Numerous graphene-based biosensing devices and techniques based on various mechanisms have been developed in the past few years^{9,14,95}. Sharing a similar chemical structure with CNTs, graphene can also be used as a drug delivery carrier^{15,16,96-98}. Recently, *in vivo* cancer treatment with graphene has been realized in animal experiments¹⁷.

Motivated by the success of CNT-based drug delivery, we researched the possibility of using graphene sheets as drug carriers for potential cancer treatment. In our two related studies in 2008^{15,16}, graphene oxide (GO) was functionalized with amine-terminated branched PEG, yielding PEGylated nano-graphene oxide (NGO-PEG) with ultra-small sizes (10 – 50 nm) and high stability in physiological solutions (Figs. 4a-c). Similar to the drug loading on CNTs, the graphene surface with delocalized π electrons can be utilized for effective loading of aromatic anticancer drugs such as doxorubicin and water-insoluble SN38 via π - π stacking (Fig. 4a). The extremely large surface area of graphene, with every atom exposed on its surface, allowed for ultra-high drug loading efficiency on NGO-PEG. The terminals of PEG chains were available for the conjugation of targeting ligands such as antibodies, which facilitated targeted drug delivery to specific types of cancer cell (Fig. 4f). Moreover, we discovered that NGO exhibited NIR photoluminescence. Although relatively weak, nano-graphene oxide NIR photoluminescence was utilized for selective imaging of cancer cells *in vitro* (Figs. 4d,e). Similar to CNTs, NGO showed strong NIR optical absorption, which was greatly enhanced following chemical reduction. The reduced NGO was targeted at cancer cells for *in vitro* NIR photothermal therapy while still maintaining biocompatibility⁷⁰. Recently, additional studies in drug loading and delivery via graphene have been reported by several groups^{96,99,100}.

Besides the delivery of small drug molecules, the latest reports suggested that functionalized graphene sheets were capable of gene transfection. In our recent work⁹⁸, negatively charged GO was non-covalently bound with cationic PEI polymers, forming GO-PEI complexes, which were stable in physiological solutions and exhibited significantly reduced cellular toxicity compared with bare PEI polymers. The positively charged GO-PEI complexes were able to further bind plasmid DNA (pDNA) for intracellular transfection of the enhanced green fluorescence protein (EGFP) gene in HeLa cells. In another independent work by Zhang *et al.*⁹⁷, GO was covalently conjugated with PEI for siRNA loading. Sequential delivery of Bcl-2 siRNA and

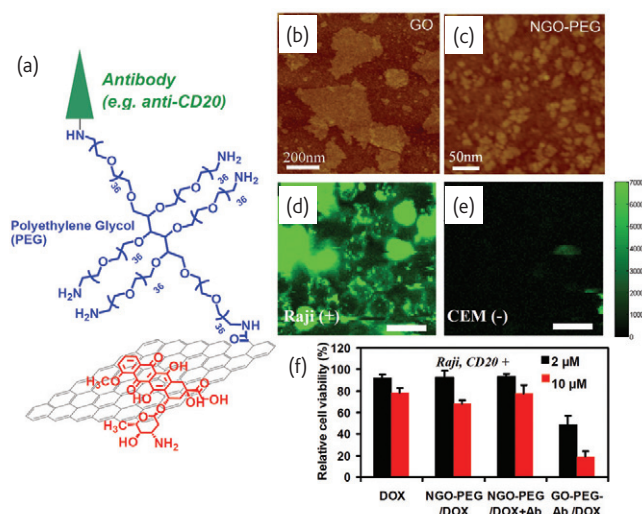


Fig. 4 Nano-graphene oxide for target cell imaging and drug delivery. (a) A schematic illustration of doxorubicin loading onto NGO-PEG-Rituxan via π -stacking. Atomic force microscopy images of as-prepared (b) GO and (c) NGO-PEG. (c). NIR fluorescence image of (d) CD20-positive Raji B-cells and (e) CD20-negative CEM cells treated with the NGO-PEG-Rituxan (anti-CD20 antibody) conjugate. Scale bar shows intensity of total NIR emission in the range of 1100 – 2200 nm under the 785 nm excitation. Scale bar = 25 μ m. (f) *In vitro* toxicity test at 2 μ M and 10 μ M DOX concentrations showing that Rituxan conjugation selectively enhanced doxorubicin delivery into Raji B-cells by comparing NGO-PEG-Rituxan/DOX with free DOX, NGO-PEG/DOX, and the mixture of DOX, Rituxan and NGO-PEG. © 2008. Reproduced with kind permission from Springer Science+Business Media and Tsinghua Press¹⁶.

doxorubicin into cancer cells by the GO-PEI conjugate showed significantly improved cell killing efficacy via a synergistic effect.

Graphene has also shown promise for *in vivo* cancer treatment in mice. To track graphene *in vivo*, we labeled PEGylated NGO with a NIR fluorescent dye for *in vivo* fluorescence imaging. Interestingly, a surprisingly high passive uptake of NGO-PEG was noticed in several different xenograft tumor models growing on mice (Fig. 5a)¹⁷. The high NIR absorption of NGO-PEG was successfully utilized for effective *in vivo* photothermal ablation of tumors (Figs. 5b-d). This was the first success of using graphene for *in vivo* cancer therapy.

Recently, a number of groups have explored the *in vivo* toxicity of graphene in animals^{17,101-103}. It was uncovered that as-prepared GO showed dominant accumulation in the lungs for long periods of time after being intravenously injected into rats or mice, inducing serious toxic effects at injection doses several-fold lower than that of NGO-PEG used in our experiments (obvious toxicity was apparent at 10 mg/kg of GO)^{101,102}. GO, without further surface functionalization, usually has sheet dimensions of hundreds of nm (Fig. 4b) and is not stable in physiological solutions with salts and proteins. On the other hand, NGO-PEG, with reduced sizes (10 – 50 nm, Fig. 4c) and significantly improved biocompatibility, showed no obvious toxic side effects to the photothermally-cured mice at a dose of 20 mg/kg within 40 days¹⁷. In another recent work¹⁰³, we found that ¹²⁵I-labeled NGO-PEG mainly localized in the liver and spleen with negligible lung accumulation after

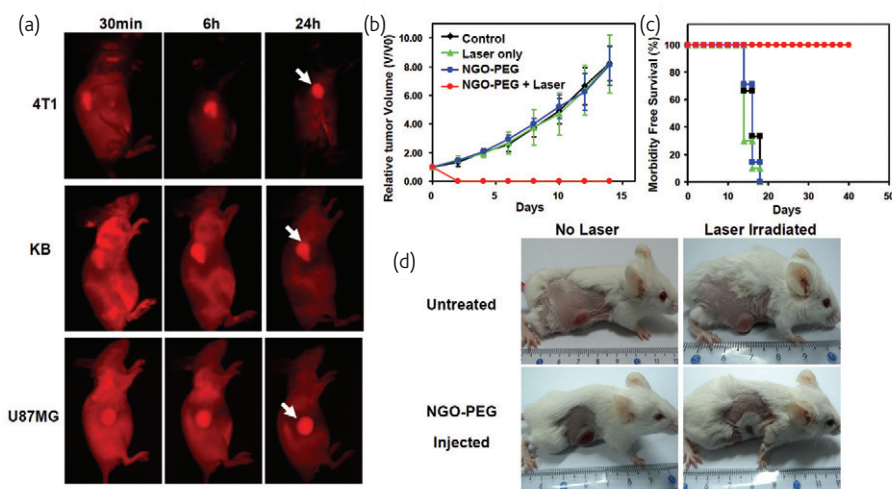


Fig. 5 Nano-graphene for in vivo photothermal therapy. (a) In vivo fluorescence images of 4T1 tumor bearing Balb/c mice, KB and U87MG tumor bearing nude mice at different time points post injection of Cy7-labeled NGO-PEG. High tumor uptake of NGO-PEG-Cy7 was observed for all of the three different tumor models. (b) Tumor growth curves of different groups of mice after graphene-based photothermal treatment. While injection of NGO-PEG by itself or laser irradiation on un-injected mice did not affect tumor growth, tumors in the treated group were completely eliminated after NGO-PEG injection and the followed NIR laser irradiation. (c) Survival curves of mice bearing 4T1 tumor after various treatments indicated. NGO-PEG injected mice after photothermal therapy survived over 40 days without any single death. (d) Representative photos of tumors on mice after various treatments indicated. The laser irradiated tumor on the NGO injected mouse was completely destroyed. Reprinted with permission from¹⁷. © 2010 American Chemical Society.

intravenous injection, and could be gradually excreted from mice. Time-course serum chemistry assays, complete blood panels, and histological examinations revealed no noticeable toxicity of NGO-PEG to the treated animals at the dose of 20 mg/kg over three months. Obviously, the *in vivo* behaviors and toxicology of graphene is highly dependent on its surface coatings, and most likely also the sheet sizes, although the latter has not yet been fully understood

Prospects and challenges

During the last decade one-dimensional carbon nanotubes have been extensively explored as nanoscale drug carriers for potential applications in cancer treatment. The unique physical properties of CNTs allow for a range of novel cancer therapies including photothermal therapy, photoacoustic therapy, and radiofrequency ablation treatment of tumors. Recently, nano-graphene has also emerged as an interesting 2D nanomaterial with promising applications in nanomedicine. Compared to other drug delivery systems, especially biodegradable organic macromolecules, inorganic nanomaterials such as CNTs and graphene may not have obvious advantages if they are simply used as drug carriers, since they hardly degrade in biological systems. However, the unique physical properties of these low-dimensional sp^2 carbon nanomaterials enable a range of novel cancer therapies (e.g., photothermal, photoacoustic, RF ablation), which could be combined with therapeutic drugs and genes co-delivered by CNTs or graphene, overcoming the multi-drug resistance problem in current cancer chemotherapies for improved tumor treatment efficacy.

How CNTs compare with graphene in nanomedicine, however, remains a question to be answered. SWNTs are 1D quantum wires

with sharp electronic density of states at the van Hove singularities that afford many intrinsic optical properties, including resonance Raman scattering and NIR photoluminescence, which are useful in biomedical imaging and imaging guided cancer therapy^{8,13,91,104-107}. Although graphene has poorer optical properties, the 2D shape and ultra-small sizes of nano-graphene (down to 10 nm and below) may offer interesting behaviors in biological systems (e.g., efficient tumor passive targeting)¹⁷. Therefore, it is still too early to determine which one among these two types of closely related sp^2 carbon nanomaterials has the greater potential for biomedical applications.

The major challenge and current limitation in this area, however, is still the potential long-term toxicity concern of graphitic nanomaterials. Although many reports have suggested that well-functionalized CNTs and nano-graphene appear to be safe to the treated animals at certain doses^{17,39,53,103}, most currently reported animal experiments are carried out on rodent models, which are different from primates and humans. The observation periods are usually no longer than six months, which may not be sufficient to determine the long-term safety of those carbon nanomaterials. Whether and how those nanomaterials affect the immune systems, reproductive systems, and nerve systems, have not yet been systematically investigated. Many more pre-clinical toxicity studies are needed before CNT- or graphene-based cancer therapies can be finally translated into the clinic. [ml](#)

Acknowledgement

This work was partially supported by a NIH-NCI R01 grant (CA135109-01) in USA, the National Natural Science Foundation of China (51002100), and a National "973" Program of China (2011CB911002).

REFERENCES

1. Kroto, H. W., et al., *Nature* (1985) **318**, 162.
2. Iijima, S., *Nature* (1991) **354**, 56.
3. Novoselov, K. S., et al., *Science* (2004) **306**, 666.
4. Dai, H., *Acc Chem Res* (2002) **35**, 1035.
5. Dresselhaus, M., and Dai, H., Eds., *MRS 2004 Carbon Nanotube Special Issue* (2004) 29.
6. Geim, A. K., *Science* (2009) **324**, 1530.
7. Loh, K. P., et al., *Nat Chem* (2010) **2**, 1015.
8. Liu, Z., et al., *Nano Res* (2009) **2**, 85.
9. Feng, L., and Liu, Z., *Nanomedicine* (2011) **6**, 317.
10. Chen, C., et al., *Nano Lett* (2005) **5**, 2050.
11. Liang, X. J., et al., *Proc Natl Acad Sci U S A* (2010) **107**, 7449.
12. Zakharian, T. Y., et al., *J Am Chem Soc* (2005) **127**, 12508.
13. Liu, Z., et al., *J Mater Chem* (2011) **21**, 586.
14. Yang, W., et al., *Angew Chem Int Ed* (2010) **49**, 2114.
15. Liu, Z., et al., *J Am Chem Soc* (2008) **130**, 10876.
16. Sun, X., et al., *Nano Res* (2008) **1**, 203.
17. Yang, K., et al., *Nano Lett* (2010) **10**, 3318.
18. Pantarotto, D., et al., *Angew Chem Int Ed* (2004) **43**, 5242.
19. Pantarotto, D., et al., *Chem Commun* (2004) 16.
20. Kam, N. W. S., et al., *J Am Chem Soc* (2004) **126**, 6850.
21. Tans, S. J., et al., *Nature* (1997) **386**, 474.
22. Kam, N. W. S., et al., *Angew Chem Int Ed* (2006) **45**, 577.
23. Jin, H., et al., *Nano Lett* (2008) **8**, 1577.
24. Heller, D. A., et al., *Adv Mater* (2005) **17**, 2793.
25. Wu, P., et al., *Angew Chem Int Ed* (2008) **47**, 5022.
26. Chen, X., et al., *J Am Chem Soc* (2006) **128**, 6292.
27. Bianco, A., et al., *Chem Commun* (2005) 571.
28. Kostarelos, K., et al., *Nat Nanotechnol* (2007) **2**, 108.
29. Kang, B., et al., *Small* (2010) **6**, 2362.
30. Mu, Q. X., et al., *Nano Lett* (2009) **9**, 4370.
31. Kam, N. W. S., et al., *Proc Natl Acad Sci USA* (2005) **102**, 11600.
32. Kam, N. W. S., and Dai, H., *J Am Chem Soc* (2005) **127**, 6021.
33. Kam, N. W. S., et al., *J Am Chem Soc* (2005) **127**, 12492.
34. Zhou, F. F., et al., *Nano Lett* (2010) **10**, 1677.
35. Jin, H., et al., *ACS Nano* (2009) **3**, 149.
36. Liu, X. W., et al., *Biomaterials* (2011) **32**, 144.
37. Prencipe, G., et al., *J Am Chem Soc* (2009) **131**, 4783.
38. Yang, S. T., et al., *Toxicol Lett* (2008) **181**, 182.
39. Liu, Z., et al., *Proc Natl Acad Sci USA* (2008) **105**, 1410.
40. Singh, R., et al., *Proc Natl Acad Sci USA* (2006) **103**, 3357.
41. Cherukuri, P., et al., *Proc Natl Acad Sci USA* (2006) **103**, 18882.
42. Wang, H. F., et al., *J Nanosci Nanotech* (2004) **4**, 1019.
43. Mutlu, G. M., et al., *Nano Lett* (2010) **10**, 1664.
44. Kolosnjaj-Tabi, J., et al., *ACS Nano* (2010) **4**, 1481.
45. Bhirde, A. A., et al., *Nanomedicine* (2010) **5**, 1535.
46. Georjina, D., et al., *J Am Chem Soc* (2009) **131**, 14658.
47. Hong, S. Y., et al., *Nat Mater* (2010) **9**, 485.
48. Welsher, K., et al., *Proc Natl Acad Sci USA* (2011) doi:10.1073/pnas.10145011108.
49. Lam, C. W., et al., *Toxicol Lett* (2004) **77**, 126.
50. Warheit, D. B., et al., *Toxicol Lett* (2004) **77**, 117.
51. Muller, J., et al., *Toxicol Appl Pharmacol* (2005) **207**, 221.
52. Poland, C. A., et al., *Nat Nanotechnol* (2008) **3**, 423.
53. Schipper, M. L., et al., *Nat Nanotechnol* (2008) **3**, 216.
54. Zhang, D. Y., et al., *Nanotechnology* (2010) **21**, 315101.
55. Bai, Y. H., et al., *Nat Nanotechnol* (2010) **5**, 683.
56. Salvador-Morales, C., et al., *Mol Immunol* (2006) **43**, 193.
57. Hamad, I., et al., *Mol Immunol* (2008) **45**, 3797.
58. Hilder, T. A., and Hill, J. M., *Nanotechnology* (2007) **18**, 175101.
59. Hilder, T. A., and Hill, J. M., *Curr Appl Phys* (2008) **8**, 258.
60. Hilder, T. A., and Hill, J. M., *Small* (2009) **5**, 300.
61. Gao, H. J., et al., *Nano Lett* (2003) **3**, 471.
62. Wu, W., et al., *Angew Chem Int Ed* (2005) **44**, 6358.
63. Pastorin, G., et al., *Chem Commun* (2006) 1182.
64. Feazell, R. P., et al., *J Am Chem Soc* (2007) **129**, 8438.
65. Dhar, S., et al., *J Am Chem Soc* (2008) **130**, 11467.
66. Liu, Z., et al., *Cancer Res* (2008) **68**, 6652.
67. Bhirde, A. A., et al., *ACS Nano* (2009) **3**, 307.
68. Liu, Z., et al., *ACS Nano* (2007) **1**, 50.
69. Ali-Boucetta, H., et al., *Chem Commun* (2008) 459.
70. Robinson, J. T., et al., *J Am Chem Soc* (2011) **133**, 6825.
71. Liu, Z., et al., *Angew Chem Int Ed* (2009) **48**, 7668.
72. Wu, W., et al., *ACS Nano* (2009) **3**, 2740.
73. Liu, Z., et al., *Nat Protoc* (2009) **4**, 1372.
74. Liu, Z., et al., *Nat Nanotechnol* (2007) **2**, 47.
75. Zerda, A. d. l., et al., *Nat Nanotechnol* (2008) **3**, 557.
76. McDevitt, M. R., et al., *J Nucl Med* (2007) **48**, 1180.
77. Singh, R., et al., *J Am Chem Soc* (2005) **127**, 4388.
78. Liu, Y., et al., *Angew Chem Int Ed* (2005) **44**, 4782.
79. Ahmed, M., et al., *Bioconj Chem* (2009) **20**, 2017.
80. Richard, C., et al., *Nano Res* (2009) **2**, 638.
81. Bartholomeusz, G., et al., *Nano Res* (2009) **2**, 279.
82. Liu, Z., et al., *Angew. Chem Int Ed* (2007) **46**, 2023.
83. Zhang, Z. H., et al., *Clin Cancer Res* (2006) **12**, 4933.
84. Chakravarty, P., et al., *Proc Natl Acad Sci USA* (2008) **105**, 8697.
85. Wang, C. H., et al., *Nanotechnology* (2009) **20**, 315101.
86. Fisher, J. W., et al., *Cancer Res* (2010) **70**, 9855.
87. Marches, R., et al., *Nanotechnology* (2011) **22**, 095101.
88. Ghosh, S., et al., *ACS Nano* (2009) **3**, 2667.
89. Burke, A., et al., *Proc Natl Acad Sci USA* (2009) **106**, 12897.
90. Moon, H. K., et al., *ACS Nano* (2009) **3**, 3707.
91. Robinson, J. T., et al., *Nano Res* (2010) **3**, 779.
92. Kang, B., et al., *Small* (2009) **5**, 1292.
93. Levi-Polyachenko, N. H., et al., *Mol Pharm* (2009) **6**, 1092.
94. Gannon, C. J., et al., *Cancer* (2007) **110**, 2654.
95. Mohanty, N., and Berry, V., *Nano Lett* (2008) **8**, 4469.
96. Zhang, L. M., et al., *Small* (2010) **6**, 537.
97. Zhang, L., et al., *Small* (2011) **7**, 460.
98. Feng, L., et al., *Nanoscale* (2011) **3**, 1252.
99. Yang, X. Y., et al., *J Phys Chem C* (2008) **112**, 17554.
100. Yang, X., et al., *J Mater Chem* (2011) doi:10.1039/C0JM02494E.
101. Wang, K., et al., *Nanoscale Res Lett* (2010) **6**, doi:10.1007/s11671-010-9751-6.
102. Zhang, X. Y., et al., *Carbon* (2010) **49**, 986.
103. Yang, K., et al., *ACS Nano* (2011) **5**, 516.
104. Liu, Z., et al., *Nano Res* (2010) **3**, 222.
105. Welsher, K., et al., *Nat Nanotechnol* (2009) **4**, 773.
106. Liu, Z., et al., *J Am Chem Soc* (2008) **130**, 13540.
107. Welsher, K., et al., *Nano Lett* (2008) **8**, 586.